Soft Matter

Accepted Manuscript

ROYAL SOCIETY OF CHEMISTRY

www.rsc.org/softmatter

Soft Matter

ARTICLE

Received 00th January 20xx,
Accepted 00th January 20xx

DOI: 10.1039/x0xx00000x

www.rsc.org/

Soft Microcapsules with Highly Plastic Shells Formed by Interfacial Polyelectrolyte-Nanoparticle Complexation

Gilad Kaufman,[a] Siamak Nejati,[a] Raphael Sarfati,[b] Rostislav Boltyanskiy,[c] Michael Loewenberg,[a] Eric R. Dufresne,[d] and Chinedum O. Osuji*[a]

Composite microcapsules have been aggressively pursued as designed chemical entities for biomedical and other applications. Common preparations rely on multi-step, time consuming processes. Here, we present a single-step approach to fabricate such microcapsules with shells composed of nanoparticle-polyelectrolyte and protein-polyelectrolyte complexes, and demonstrate control of the mechanical and release properties of these constructs. Interfacial polyelectrolyte-nanoparticle and polyelectrolyte-protein complexation across a water-oil droplet interface results in the formation of capsules with shell thicknesses of a few µm. Silica shell microcapsules exhibited a significant plastic response at small deformations, whereas lysozyme incorporated shells displayed a more elastic response. We exploit the plasticity of nanoparticle incorporated shells to produce microcapsules with high aspect ratio protrusions by micropipette aspiration.

[a] Department Of Chemical and Environmental Engineering
Yale University, New Haven, CT, 06511
[b] Department of Applied Physics, Integrated Graduate Program in Physical and Engineering Biology
Yale University, New Haven, CT, 0651.
[c] Department of Physics Yale University, New Haven, CT,USA
[d] Department of Mechanical Engineering and Material Science
Yale University, New Haven, USA

Electronic Supplementary Information (ESI) available: [Materials, capsule diameter as a function of flow rate, UV-Vis measurements]. See DOI: 10.1039/x0xx00000x

1 Introduction

The fabrication of microcapsules as a vehicle for cargo storage and controlled release in biomedical applications,[1, 2] food science,[3] and personal care products,[4] is of ever increasing importance. Various techniques have been developed and optimized for the fabrication of capsules with tailored structures and properties including polymerization induced phase separation,[5] double emulsion templating,[6] and the layer-by-layer (LbL) assembly.[7] The LbL method involves sequential deposition of polyelectrolyte layers based on electrostatic interactions onto a sacrificial template followed by the removal of the template. Nanoparticles have been incorporated into the shells of LbL capsules to manipulate properties such as mechanical stability,[8] permeability,[9] and responsiveness to external stimuli.[10] While LbL is greatly versatile in fabricating composite nanoparticle-polyelectrolyte capsules, it is a multi-step and therefore, a time-consuming approach. An alternative to LbL for nanoparticle incorporation in microcapsule shells involves direct adsorption of colloidal particles onto oil-water interfaces, resulting in Pickering emulsions. Such an approach, however, lacks the versatility of LbL and requires careful control of particle wettability to allow control over the type of capsules generated (water core or oil core) and to ensure their stability.[11]

A hybrid approach can be envisioned, in which electrostatic interactions between particles and polymers at the oil-water interface of an emulsion droplet are used to form a particle-polymer complex at the droplet shell. The ability of polyelectrolyte pairs and other complementary species to associate at oil-water interfaces [12-14] suggests the viability of the hybrid approach, but no particle-polymer based microcapsules have been fabricated in this manner to date. An approach suggested here would provide a simple and fast method to generate composite microcapsules, as well as the ability to modify the permeability and mechanical properties of the microcapsule by modifying the composition and identity of shell constituents.

Here, we present a one-step microfluidic approach for generating soft composite polyelectrolyte microcapsules using interfacial complexation across an oil-water interface. We show that these microcapsules can be generated based on the associative interactions of a polyelectrolyte and positively charged nanoparticles or proteins. We choose silica nanoparticles and lysozyme protein as model materials. We examine the mechanical and release behavior of microcapsules fabricated with silica particles and show that

the stiffness of the capsule and the release behavior can be controlled by varying the concentration of the nanoparticles used in the aqueous phase during capsule fabrication. Finally, we highlight the highly plastic nature of the silica shell capsules compared to lysozyme shell capsules when subjected to deformation by micropipette aspiration.

2 Experimental details

2.1 Synthesis of amine modified silica nanoparticles

We followed a procedure from Mahalingam *et al.*[15] Briefly bare silica nanoparticles roughly 50 nm in diameter were synthesized by mixing 3.8 ml of tetraethyl orthosilicate, 5.7 ml of ammonium hydroxide, and 114 ml of ethanol in a glass flask while stirring for 3 hours at room temperature. The nanoparticles were purified by repeated cycles of centrifugation and washing steps. Fluorescein isothiocyanate (FITC) precursor solution was prepared by mixing 0.0135 mmol of FITC and 0.385 mmol of (3-aminopropyl)triethoxysilane in ethanol while stirring overnight in the dark at room temperature. To label the nanoparticles, 1 ml of the precursor solution was added to 50 ml of the bare nanoparticles solution and left stirring for 2 hours, followed by the above purification steps. Finally, the amine modified silica nanoparticles were dried in an oven at 80 ° C for 3 hours.

2.2 Labeling of lysozyme with FITC

Labeling of lysozyme with FITC was performed using an adapted procedure based on that of Kok *et al.*[16] 4.25 x 10^{-5} wt.% of FITC and 1.5 wt.% of lysozyme were dissolved in 0.1 M borate buffer (pH 9.1) and stirred for 4 hours at room temperature in the dark. The pH of the solution was then adjusted to 7.4 using 3 M hydrochloric acid, and the solution was dialyzed for 72 hours in a fridge set to 5 °C against a mixture of 2 mM (4-(2-hydroxyethyl)-1-piperazineethanesulfonic acid) buffer (HEPES buffer) and 0.1 mM ethylenediaminetetraacetic acid (EDTA).

2.3 Dye-loaded microcapsules

In a typical experiment, 0.012 mM of the dye (Oil Blue N) in a 96.2/3.8 % by volume of ethanol/water solution containing 0.1, 0.25 or 0.5 wt.% of positively charged alumina coated silica nanoparticles (LUDOX-CL) served as the core of the microcapsules. The outer phase was 0.3 wt.% sulfonated styrene copolymer (s-SEBS) in toluene

3 Results and Discussion

Microcapsules with aqueous cores were prepared by generating a water-in-oil (w/o) emulsion in a capillary microfluidic device using standard procedures, as described elsewhere.[17] The emulsion droplets contained positively charged alumina coated silica nanoparticles or lysozyme in water, while the outer phase was a solution of a sulfonated styrene copolymer in toluene. The positive charge on the nanoparticles originates from the protonation of the hydroxylated oxide surface, with $Al(OH)_2^+$ groups present below the isoelectric point.[18] The silica nanoparticles have a nominal diameter of 21 nm and an isoelectric point of ~ 8.7.[19, 20] The small but finite solubility of s-SEBS in the water phase allows s-SEBS chains to diffuse across the oil-water interface into the aqueous droplet interior where its sulfonate moieties become charged.[13] The negatively charged sulfonate groups interact electrostatically with the positively charged $Al(OH)_2^+$ groups of the silica nanoparticles and form an ionic complex using the oil-water interface as a scaffold. Schematic illustrations of the microfluidic device and the microcapsule shell formation are shown in Figures 1a and 1b, respectively.

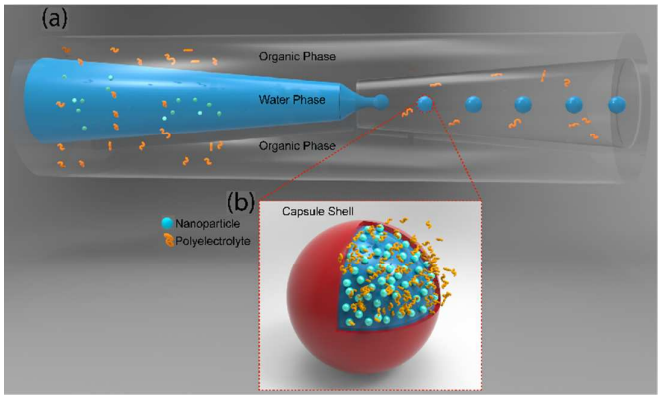

Fig. 1 (a) Schematic of a glass capillary microfluidic device used for polyelectrolyte-nanoparticle microcapsule fabrication from w/o emulsion templates (blue drops) (b) Shell formation through electrostatic interactions between the charged nanoparticles (turquoise) and polyelectrolyte (orange) across the water-oil interface

Microcapsules with various diameters ranging from 170 to 250 µm were produced with ~ 3% polydispersity by varying the relative flow rates of the dispersed and continuous phases per standard practice (Supporting Information, Figure S1).[21] A representative image of a monodisperse collection of microcapsules is shown in Figure 2a.

The formation of capsules is evident by the wrinkles developed on the object's surface upon drying, as shown in Figure 2b. The thickness of the microcapsule shell was measured using scanning electron microscopy (SEM). Individual capsules were freeze fractured, followed by rapid drying at 80 °C. Cross-sectional imaging of the microcapsules, Figure 2c, shows the capsule shell is about 3 µm thick with nanoparticles dispersed throughout. This large shell thickness relative to the dimensions of the constituent species suggests that the shell formation involves simultaneous inter-diffusion and complexation of the components with the process arresting at a critical point, where the density of the formed complex inhibits further mass transport.

It is apparent that the shell contains nanoparticles coated by the polymer in a dense thick layer. Confocal microscopy images using fluorescently labeled silica nanoparticles confirm

this, with strong fluorescence emanating from the shell region and shown in Figure 3.

Microcapsules were fabricated in the second series of experiments using lysozyme in lieu of the silica nanoparticles. Lysozyme is a globular protein and exists as a roughly spherical object with a hydrodynamic diameter of ~ 4 nm, and isoelectric point of 11.4.[22, 23] The protein was fluorescently labeled with FITC. Phase contrast and the corresponding fluorescent confocal image, Figures 3c and 3d, show the accumulation of labeled lysozyme at the droplet interface, as evident from the strong fluorescence signal. The shell thickness for the silica and lysozyme based capsules was measured using a previously established procedure as the full-width at half-maximum of Gaussian fits of fluorescence intensity profiles across the shell.[13] We note here that capsules were also successfully obtained using silica nanoparticles, as well as lysozyme, under fairly high ionic strength conditions of 1M NaCl, with 0.3 wt.% SEBS and 0.3 wt.% of silica or lysozyme. It is possible that electrostatic interactions are not the only reason for complex formation. We do not rule out the possibility that hydrophobic associations, or hydrogen bonding, between the sulfonate acceptor of SEBS and the donor hydroxyl groups of silica and lysozyme, may also play a role.

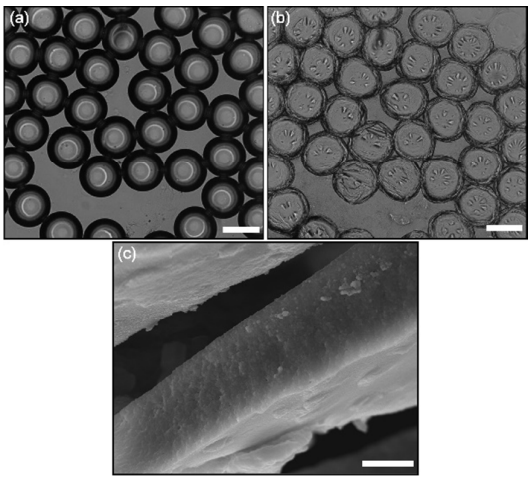

Fig. 2 (a) Optical micrograph showing monodisperse silica/s-SEBS microcapsules with diameter of 248.0 ± 4.4 µm before drying (b) Formation of wrinkles on the microcapsules surface after drying for 30 minutes on a glass slide. Scale bar is 200 µm. (c) Scanning electron micrograph of dried microcapsules shows nanoparticle-polymer shell film with µm size thickness. Scale bar is 2.5 µm

The mechanical properties of silica and lysozyme based capsules were probed by observing capsule deformation and recovery during and after pressure driven passage through a tapered capillary, Figure 4. Details of the experimental setup were described previously.[13] Application of pressure resulted in deformation of the initially spherical capsules into ellipsoids as the capsule moved down the tapered capillary. The elasticity of the shells was evaluated by the ability of the capsules to recover to spherical shapes as reflected by, Δ(AR) in Equation 1, the change in their aspect ratios relative to their isotropic starting point on release of the deformation-inducing pressure or exit of the capsule from the capillary.

$$\Delta(AR) = \frac{a}{b} - \frac{A}{B} \quad (1)$$

Additionally, the strength of the silica-based microcapsule shells was assessed based on the pressure required to induce concave-to-convex buckling of the upstream or pressure-facing spherical cap, at a fixed point during the deformation of the object, Figures 4h and 4j.

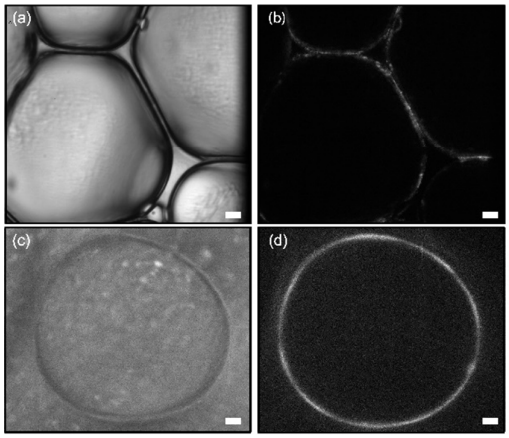

Fig. 3 (a) Bright-field micrograph of fluorescently labeled amine modified silica/s-SEBS microcapsules on a glass slide covered by a cover slip. (b) Corresponding confocal micrograph of the microcapsules showing preferential packing of the fluorescently labeled silica nanoparticles at capsule interface. *Capsule shell is ~2 µm.* (c) Phase contract image of lysozyme/s-SEBS microcapsules on a glass slide. (d) Corresponding lysozyme/s-SEBS microcapsules on a glass slide showing accumulation of fluorescently labeled lysozyme at the capsule interface. *Capsule shell is ~3 µm.* Scale bar is 20 µm.

As shown in Figure 4, silica-based microcapsules that were elongated to an aspect ratio of ~ 1.80 recovered to an aspect ratio of ~ 1.40, with Δ(AR) ~ 0.38. By contrast, lysozyme based microcapsules recovered almost completely, from ~ 1.80 to ~ 1.02, with Δ(AR) values an order of magnitude smaller compared to silica-based microcapsules (Δ(AR) ~ 0.02). The substantial difference in the elasticity of the silica and lysozyme microcapsules is striking, although the precise reasons are not clear. It may reflect differences in the interaction strengths of lysozyme with s-SEBS compared to silica nanoparticles, or differences in the ability of lysozyme as a globular protein to accommodate deformation relative to the rigid silica. Additional work on this topic is warranted. It is worthwhile to note that plastic deformation has been observed in supracolloidal architectures such as Pickering emulsions[24, 25] and armored bubbles.[26] In those systems, the absence of surface-tension driven shape recovery is linked to the jamming of colloidal particles at the interface, with additional particles recruited to the interface when the objects are deformed. In the present scenario, we find it unlikely that

the formation of new shell material on deformation of capsule occurs here despite a finite concentration of s-SEBS in the suspending fluid during deformation. It is our assertion that instead, the shell material simply yields to accommodate the increase in surface area, with a concomitant reduction in shell thickness.

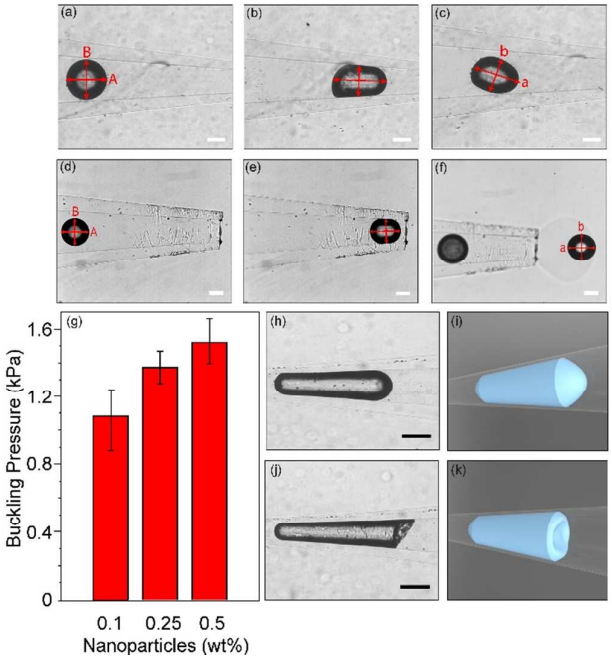

Fig. 4 (a)-(f) Bright-field optical microscopy images showing deformation of microcapsules. (a) silica/s-SEBS microcapsule before deformation with an initial aspect ratio (A/B) of 1. (b) The microcapsule deforms as the pressure is increased to 450 Pa with an aspect ratio of 1.77 (c) The microcapsule retains its non-spherical shape upon reversal of the applied pressure with final aspect ratio (a/b) of 1.38. (d) Lysozyme/s-SEBS microcapsule morphology before deformation with an initial aspect ratio (A/B) of 1 (e) The pressure is increased to 385 Pa and the microcapsule deforms to an aspect ratio of 1.76. (f) The microcapsule recovers its initial spherical shape after transiting the capillary with a final aspect ratio (a/b) of 1.02. A plume is visible as the capsule exits due to slight differences in the index of refraction of the capsule suspension and test bath fluids. Scale bar is 100 μm. (g)-(k) Determination of silica/s-SEBS microcapsule buckling pressure. (g) Buckling pressure as a function of nanoparticle concentration. (h) Microcapsules deformed in a tapered capillary before buckling. (i) Schematic illustration showing deformed microcapsule corresponding to (h). (j) Representative image showing buckling of the upstream surface of the microcapsules. (k) Schematic illustration of microcapsule buckling shown in (j). All scale bars are 100 μm. The capillary is tapered to 72 μm with a taper angle of 8º.

The silica-based microcapsules display a clear dependence of their mechanical properties on composition, with an increase in buckling pressure from ~ 1100 Pa to ~ 1500 Pa on increasing nanoparticle concentration from 0.1 to 0.5 wt.%. These measurements indicate that the mechanical integrity of the microcapsules improves as higher nanoparticles concentration is used for the shell formation. We can account for this in a straightforward fashion as microcapsules prepared with higher nanoparticle concentration presumably have a denser and thicker microcapsule shell which would require a larger pressure to buckle. This is from the perspective that denser and thicker nanoparticle-polymer shells have improved mechanical properties.[27] Similar trends have also been noted by Teixeira *et al.* for polydimethylsiloxane microcapsules decorated with nanoparticles.[28]

The plastic deformation of the silica-based microcapsules was explored as a potential route to form microcapsules with complex or unusual topology using micropipette aspiration, Figure 5. A tapered capillary with an end-diameter significantly smaller than that of the microcapsule was brought into contact with the capsule surface. A small suction pressure was then applied, causing aspiration of the microcapsule shell into the pipette. The local deformation produced by the aspiration persisted on removal of the suction pressure, resulting in the formation of an elongated bleb-like protrusion from the capsule surface. As shown in Figure 5f, such local deformations could be performed repeatedly, here, 5 times, at different locations of the microcapsule's surface, producing a final complex shape featuring multiple high aspect protrusions. Notably, the protrusions and the capsules showed no signs of instability related to their deformation. They remained stable over the entire course of the experiment (~ 30 minutes). The reduced optical density of the protrusions relative to the non-deformed capsule areas is consistent with the shell yielding hypothesis described earlier.

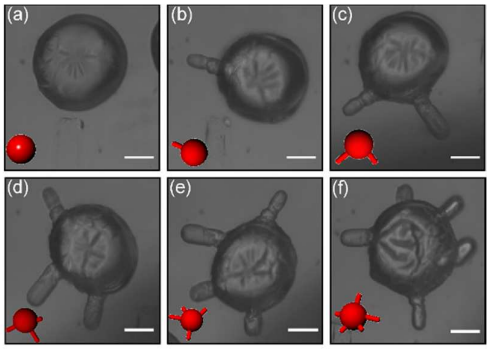

Fig. 5 Optical micrographs showing microcapsule with multiple protrusions formed by micropipette aspiration. An aspiration pressure of 2-5 cm of water is applied to aspirate the microcapsule into the capillary. Upon release of the pressure, the protrusion remains stable, and the micropipette is moved away from the capsule. (a) Microcapsule before aspiration, (b)-(e) series of aspiration experiments showing formation of additional protrusions after each aspiration. Scale bar is 50 μm

Based on the ability to tailor the mechanical properties of the microcapsules, it is expected that the nanoparticle concentration will also affect the permeability of the microcapsule shell. The ability to tune the shell permeability is highly desirable for controlled release applications.[28, 29] We investigated this by encapsulating a dye, Oil Blue N, in the aqueous core of microcapsules suspended in toluene. The diffusion of the dye through the microcapsule shell was monitored as a function of time using UV-Vis spectroscopy measurements to recover the concentrations (Supporting Information, Figure S2). Data were fitted to a one dimensional

equation describing radial diffusion through a spherical shell, Equation 2.

$$\frac{C_t}{C_\infty} = 1 - e^{-At} \quad (2)$$

Here, $A = 3D/rh$, D is the diffusivity of the dye, r is the microcapsule radius, and h is the shell thickness. C_t is the time dependent concentration in the toluene while C_∞ is the long time value, i.e. after complete release. The results, Figure 6, show that there is an inverse correlation between nanoparticle concentration, c_{np}, and release rate, $A \sim 1/c_{np}$.

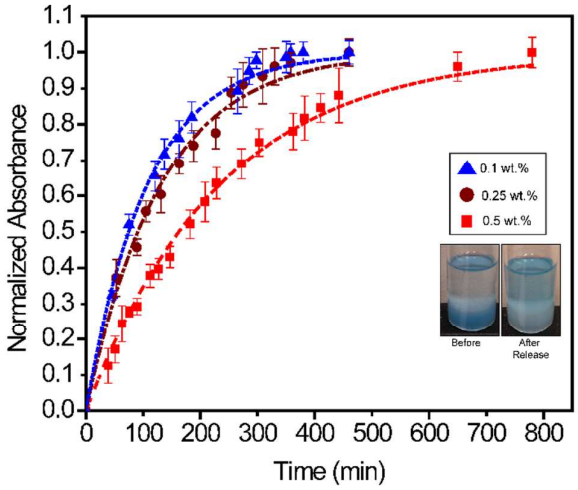

Fig. 6 Time dependent release of Oil Blue N dye from silica/s-SEBS nanoparticles shells microcapsules core for different nanoparticles concentration used in microcapsules preparation. Blue triangles, brown circles, and red squares represent normalized dye concentration (measured concentration/final concentration), for 0.5, 0.25, and 0.1 wt.% of silica nanoparticles in the aqueous phase, respectively. The fitting parameter (A) describing the microcapsule permeability was 4.3 x 10^{-3} min^{-1}, 7.7 x 10^{-3} min^{-1}, and 9.3 x 10^{-3} min^{-1} for 0.5, 0.25, and 0.1 wt.% of silica. Inset shows images before and after the dye release from the microcapsules. Error bars represent the standard deviation of multiple short duration measurements at each time point.

The results demonstrate that the diffusion of the dye through the silica/s-SEBS shell can be readily controlled by varying the nanoparticle concentration in the aqueous solution during microcapsule formation. This is consistent with the expected release behavior of nanoparticle-decorated microcapsules that show slower release for capsules prepared with higher nanoparticle concentrations.[28]

4 Conclusions

In summary, we have presented a facile, single-step microfluidic approach to fabricate nanoparticle-polyelectrolyte and protein-polyelectrolyte composite microcapsules using w/o emulsion droplets as templates. The microcapsules thus formed are mechanically stable and feature shells with thicknesses on the order of a few µm. We observe striking differences in the elasticity of shells prepared from silica nanoparticles compared to those prepared from a globular protein, lysozyme. The plastic deformability of silica-based shells was exploited to generate microcapsules with complex shapes using pipette aspiration. We demonstrated that the mechanical integrity and permeability of the silica-based microcapsules could be rationally manipulated by controlling the concentration of nanoparticles used during microcapsule fabrication. Taken together, these results offer a new route for fabricating composite microcapsules with potentially useful mechanical, release and other functions.

Acknowledgements

This work was supported by NSF under CBET-1066904. C.O. acknowledges support from a 3M Nontenured Faculty Award. Facilities use was supported by YINQE and NSF MRSEC DMR-1119826. We acknowledge Dr. Rachid Thiam for helpful discussions.

Notes and references

1. B. G. De Geest, S. De Koker, G. B. Sukhorukov, O. Kreft, W. J. Parak, A. G. Skirtach, J. Demeester, S. C. De Smedt and W. E. Hennink, *Soft Matter*, 2009, **5**, 282-291.
2. A. Sergeeva, D. Gorin and D. Volodkin, *BioNanoSci.*, 2014, **4**, 1-14.
3. S. Je Lee, *J. Food Sci. Technol.*, 2000, **33**, 80-88.
4. A. Ammala, *Int. J. Cosmet. Sci.*, 2013, **35**, 113-124.
5. P. J. Dowding, R. Atkin, B. Vincent and P. Bouillot, *Langmuir*, 2005, **21**, 5278-5284.
6. S. S. Datta, A. Abbaspourrad, E. Amstad, J. Fan, S.-H. Kim, M. Romanowsky, H. C. Shum, B. Sun, A. S. Utada, M. Windbergs, S. Zhou and D. A. Weitz, *Adv. Mater.*, 2014, **26**, 2205-2218.
7. G. Decher, *Science*, 1997, **277**, 1232-1237.
8. M. F. Bedard, A. Munoz-Javier, R. Mueller, P. del Pino, A. Fery, W. J. Parak, A. G. Skirtach and G. B. Sukhorukov, *Soft Matter*, 2009, **5**, 148-155.
9. A. San Miguel and S. H. Behrens, *Soft Matter*, 2011, **7**, 1948-1956.
10. H. Duan and S. Nie, *J. Am. Chem. Soc.*, 2007, **129**, 2412-2413.
11. B. P. Binks and S. O. Lumsdon, *Langmuir*, 2000, **16**, 8622-8631.
12. S. Le Tirilly, C. Tregouët, S. Bône, C. Geffroy, G. Fuller, N. Pantoustier, P. Perrin and C. Monteux, *ACS Macro Lett.*, 2015, **4**, 25-29.
13. G. Kaufman, R. Boltyanskiy, S. Nejati, A. R. Thiam, M. Loewenberg, E. R. Dufresne and C. O. Osuji, *Lab Chip*, 2014, **14**, 3494-3497.
14. H. Monteillet, F. Hagemans and J. Sprakel, *Soft Matter*, 2013, **9**, 11270-11275.
15. V. Mahalingam, S. Onclin, M. Péter, B. J. Ravoo, J. Huskens and D. N. Reinhoudt, *Langmuir*, 2004, **20**, 11756-11762.
16. R. J. Kok, M. Haas, F. Moolenar, D. de Zeeuw, and D. K. F. Meijer, *Ren. Fail.*, 1998, **2**, 211 - 217.
17. A. S. Utada, E. Lorenceau, D. R. Link, P. D. Kaplan, H. A. Stone and D. A. Weitz, *Science*, 2005, **308**, 537-541.
18. M. Robinson, J. A. Pask and D. W. Fuerstenau, *J. Am. Ceram. Soc.*, 1964, **47**, 516-520.

19. C.-D. Vo, A. Schmid, S. P. Armes, K. Sakai and S. Biggs, *Langmuir*, 2007, **23**, 408-413.
20. M. Stępnik, J. Arkusz, A. Smok-Pieniążek, A. Bratek-Skicki, A. Salvati, I. Lynch, K. A. Dawson, J. Gromadzińska, W. H. De Jong and K. Rydzyński, *Toxicol. Appl. Pharmacol.*, 2012, **263**, 89-101.
21. R. K. Shah, H. C. Shum, A. C. Rowat, D. Lee, J. J. Agresti, A. S. Utada, L.-Y. Chu, J.-W. Kim, A. Fernandez-Nieves, C. J. Martinez and D. A. Weitz, *Mater. Today*, 2008, **11**, 18-27.
22. C. C. F. Blake, D. F. Koenig, G. A. Mair, A. C. T. North, D. C. Phillips and V. R. Sarma, *Nature*, 1965, **206**, 757-761.
23. L. R. Wetter and H. F. Deutsch, *J. Biol. Chem.*, 1951, **192**, 237-242.
24. S. A. F. Bon, S. D. Mookhoek, P. J. Colver, H. R. Fischer and S. van der Zwaag, *Eur. Polym. J.*, 2007, **43**, 4839-4842.
25. M. Cui, T. Emrick and T. P. Russell, *Science*, 2013, **342**, 460-463.
26. A. Bala Subramaniam, M. Abkarian, L. Mahadevan and H. A. Stone, *Nature*, 2005, **438**, 930-930.
27. C. Gao, E. Donath, S. Moya, V. Dudnik and H. Möhwald, *Eur. Phys. J. E*, 2001, **5**, 21-27.
28. R. F. A. Teixeira, O. van den Berg, L.-T. T. Nguyen, K. Fehér and F. E. Du Prez, *Macromolecules*, 2014, **47**, 8231-8237.
29. G. Ibarz, L. Dähne, E. Donath and H. Möhwald, *Chem. Mater.*, 2002, **14**, 4059-4062.

Graphical Abstract

Soft Microcapsules with Highly Plastic Shells Formed by Interfacial Polyelectrolyte-Nanoparticle Complexation

Gilad Kaufman,[a] Siamak Nejati,[b] Raphael Sarfati,[c] Rostislav Boltyanskiy,[d] Michael Loewenberg,[a], Eric R. Dufresne,[d] and Chinedum O. Osuji[a]*

We present a single-step microfluidic approach to fabricate soft microcapsules with shells composed of nanoparticle-polyelectrolyte and protein-polyelectrolyte complexes, and demonstrate control of the mechanical and release properties of these constructs.